Published in final edited form as:
Biochem Biophys Res Commun. 2007 January 26; 352(4): 843–849. doi:10.1016/j.bbrc.2006.11.071.

A comparison of substrate dynamics in human CYP2E1 and CYP2A6

John P. Harrelson[a,*], **Kirk R. Henne**[b], **Darwin O.V. Alonso**[a], and **Sidney D. Nelson**[a]

[a] Department of Medicinal Chemistry, University of Washington, Box 357610, Seattle, WA 98195

[b] Amgen Incorporated, Thousand Oaks, CA 91320

Abstract

Considering the dynamic nature of CYPs, methods that reveal information about substrate and enzyme dynamics are necessary to generate predictive models. To compare substrate dynamics in CYP2E1 and CYP2A6, intramolecular isotope effect experiments were conducted, using deuterium labeled substrates: *o*-xylene, *m*-xylene, *p*-xylene, 2,6-dimethylnaphthalene, and 4,4′-dimethylbiphenyl. Competitive intermolecular experiments were also conducted using d_0- and d_6-labeled *p*-xylene. Both CYP2E1 and CYP2A6 displayed full isotope effect expression for *o*-xylene oxidation and almost complete suppression for dimethylbiphenyl. Interestingly, $(k_H/k_D)_{obs}$ for d_3-*p*-xylene oxidation ($(k_H/k_D)_{obs}$ = 6.04 and $(k_H/k_D)_{obs}$ = 5.53 for CYP2E1 and CYP2A6, respectively) was only slightly higher than $(k_H/k_D)_{obs}$ for d_3-dimethylnaphthalene ($(k_H/k_D)_{obs}$ = 5.50 and $(k_H/k_D)_{obs}$ = 4.96, respectively). One explanation is that in some instances $(k_H/k_D)_{obs}$ values are generated by the presence of two substrates bound simultaneously to the CYP. Speculatively, if this explanation is valid, then intramolecular isotope effect experiments should be useful in the mechanistic investigation of P450 cooperativity.

Keywords

CYP2E1; CYP2A6; Isotope effect; Cooperativity; Allosterism; Dynamics; P450; k_H/k_D; Xylene

Some Cytochromes P450 (CYP or P450) catalyze the oxidative metabolism of exogenous compounds, including drugs, to metabolites that are usually less toxic and more water soluble, especially after conjugation. This process is important since it reduces the risk of drug-induced toxicity by facilitating drug elimination. However, in certain cases, CYP-catalyzed oxidation may also lead to the formation of reactive, electrophilic metabolites that can lead to toxicity or carcinogenicity. Inhibition or induction of specific P450 isoforms can also be a source of drug-drug interactions. On account of these important roles that CYPs play in drug metabolism and drug toxicity, a substantial effort to characterize the drug-metabolizing CYPs continues with hopes of predicting such details as isoform selectivity of new drug candidates, rates of metabolite formation, product selectivity, and the formation of toxic metabolites.

The development of accurate predictive models requires, among other things, an understanding of structure (both of the enzyme and the substrate), mechanism, and kinetics. With CYP

*Corresponding author: Fax: 503 352 7270, E-mail address: harrelsonj@pacificu.edu.

enzymes a clear understanding of this relationship is especially challenging since there is the additional complexity that, in many instances, a single enzyme can bind a variety of substrates, multiple substrates, and/or generate multiple products from a single substrate. A variety of tools have been used to investigate P450 structure including x-ray crystallography, mechanism-based inactivators, photoaffinity labeling, site directed mutagenesis, and homology modelling. These techniques have been effective in the identification of residues that are important for function [1], substrate selectivity [2], product selectivity [3], and cooperative kinetics [4]. Interestingly, the *static* crystal structures of modified human CYPs have provided insight into the *dynamic* nature of the CYPs. In some structures the substrate is positioned so far away from the heme that some motion or translation by the substrate and/or protein is required for substrate oxidation [5]. In other cases, the structural changes observed in comparisons of the substrate-free versus substrate-bound structures are indicative of significant protein motion [6;7]. Therefore, considering the dynamic nature of CYPs, methods that reveal information concerning substrate and CYP dynamics are crucial for understanding mechanisms of substrate binding and orientation, product selectivity, multiple ligand binding, and ultimately, accurate predictive models.

Currently there are several tools that can provide information about CYP and substrate dynamics. CO-flash photolysis has been effective at revealing information about the overall flexbility of P450 enzymes [8]. Fluorescence studies have also been used to investigate protein dynamics [9;10;11]. Solid-state NMR was recently used to investigate amino acid motion upon substrate binding in $P450_{BM-3}$ [12]. A solid-state NMR method was also used to study $P450_{cam}$ and provided evidence that the substrate, adamantane, undergoes rapid motion within the P450cam active site [13]. In the current study we have used deuterium isotope effect experiments to investigate substrate dynamics.

For more than thirty years investigators have utilized deuterium isotope effect experiments to study CYP enzymes. Because of the mechanistic information that deuterium isotope effect experiments can provide, initially much of this work focused on understanding the steps of substrate oxidation (e.g., H atom abstraction versus oxygen insertion) and utilized both intermolecular and intramolecular deuterium isotope effect experiments [14;15;16]. Stimulated by the earlier mechanistic experiments it became apparent that information about substrate dynamics could be revealed using intramolecular isotope effect experiments that utilize a series of symmetrical and selectively deuterium labeled substrates [17;18;19]. The technique takes advantage of the isotope effect suppression (the masking effect) that is observed when the rate of interchange between labeled and unlabeled regions of a molecule is slow compared to the rate of product formation. The technique involves using a series of symmetrical compounds like those shown in Figure 1, where one methyl group is labeled (R-CD_3) and the other is unlabeled (R-CH_3) with increasing separation between the symmetrically-related groups. Full expression of the isotope effect is expected for compounds that can reorient rapidly in the active site (i.e., short distances between methyl groups). However as the methyl group separation is increased the enzyme active site structure hinders substrate reorientation and the intrinsic isotope effect is suppressed. That is, the observed isotope effect is smaller than the intrinsic isotope effect. Theoretically, in cases of multiple ligand binding (P450 allosterism), a second substrate could also lead to changes in substrate dynamics and changes in the observed isotope effect [20]. Therefore, for a given CYP isoform, the isotope effect suppression profile across the series of substrates can provide two pieces of information. It can convey information about substrate motion, that is, the rate of interchange between labeled and unlabeled groups, and how this rate of interchange changes with different substrates for a single enzyme or, alternatively, how the rate of interchange changes from isoform to isoform using an identical substrate. Secondly, in circumstances where a single substrate binds to the enzyme it can provide an estimate of the active site area and volume available for unhindered substrate rotation [21].

CYP2E1 and CYP2A6 are good candidates for comparative studies that focus on the relationship between substrate dynamics and enzyme structure. In addition to belonging to the same CYP2 family, they share a rather broad overlap in substrate selectivity (e.g., dimethylnitrosamine, diethynitrosamine, *p*-nitrophenol, halothane, acetaminophen, and butadiene) and both are widely assumed to have relatively small active sites because of their preference for low molecular weight substrates [2;22;23;24;25;26;27;28;29;30;31;32]. In some instances each enzyme displays unique product selectivity for the same substrate. For example, with acetaminophen the predominant metabolite of CYP2E1 mediated oxidation is *N*-acetyl-*p*-quinoneimine (NAPQI). Meanwhile, CYP2A6 predominantly catalyzes the formation of the relatively non-toxic catechol [33]. In the work presented here, the CYP2E1 and CYP2A6 active sites were probed using symmetrical intramolecular and competitive intermolecular isotope effect experiments in order to assess substrate dynamics and the active site space of these isoforms. We also hoped to identify some significant differences in the k_H/k_D suppression profile that could be exploited in the future using a combination of reciprocal mutagenesis and isotope effect experiments to identify active site residues that affect substrate dynamics.

Materials and methods

o-Xylene-α-$^2H_3$, 4-$2H_3$,4′-dimethylbiphenyl, and 2-$^2H_3$,6-dimethylnaphthalene were synthesized as described previously [18;21]. Supersomes™ (human CYP2E1 and human CYP2A6 with P450 reductase and cytochrome b5) and insect cell control microsomes were from BD Gentest. *p*-Xylene, *p*-xylene-α, α, α, α′, α′, α′-d_6, methyl 3-methylbenzoate, methyl 4-methylbenzoate, lithium aluminum deuteride (LAD), methanesulfonyl chloride, N,N-diisopropylethylamine (EDIPA), pentane, BSTFA, and NADPH, were purchased from Sigma-Aldrich. Methanol was purchased from Fisher. DB-5 gas chromatography capillary column was from J&W Scientific, (Folsom, CA). Econosil C18 column was purchased from Alltech.

Synthesis and Characterization of p-Xylene-α-$^2H_3$

This compound was synthesized and purified as described previously [18] with minor changes. Methyl 4-methylbenzoate (7.6 g, 0.05 mol) in ether was added dropwise to LAD (2.4 g, 0.05 mol) suspended in ether and magnetically stirred overnight under nitrogen, at room temperature. The reaction was quenched cautiously with 1 mL water, 2 mL 15% NaOH, and then again with water to ensure complete decomposition. The reaction mixture was filtered and extracted several times with pentane. The combined pentane layers were dried with sodium sulfate and then evaporated and dried further in vacuo to yield white needle-like crystals of *p*-methylbenzylalcohol (5.5 g, 0.045 mol, 90% yield, m.p. = 56–59 °C). A portion of the alcohol (3.2 g, 0.026 mol) was stirred overnight with methane sulfonylchloride (6.4 g, 0.056 mol) in 150 mL dichloromethane containing 16.5 mL EDIPA. The reaction mixture was washed two times with 150 mL water and two times with 150 mL saturated sodium bicarbonate. The organic layer was dried with sodium sulfate and evaporated. The mesylate was purified on an alumina column (2.5 cm × 44 cm, activated, neutral, Brockman I) with pentane as the elution solvent. Pentane was removed by rotoevaporation to yield the pure *p*-methylbenzyl mesylate (faint yellow oil, 2.4 g, 0.012 mol, 45% yield). The mesylate (1.3 g, 0.0062 mol) was dissolved in 25 mL dry tetrahydrofuran (THF) and added dropwise to LAD (0.28 g, 0.0067 mol) suspended in 10 mL THF and then magnetically stirred overnight with gentle reflux and a nitrogen soft cap. The reaction was quenched as described above for the alcohol, extracted with pentane, and dried with sodium sulfate. The xylene was transferred to a flask equipped with a water-cooled condenser, placed in a dry ice/isopropyl alcohol bath and then concentrated with a stream of air. The *p*-xylene-α-$^2H_3$ was purified on an alumina column (2.5 cm × 21.5 cm) using pentane, which was distilled off to yield the pure compound (0.50 g, 0.0046 mol, 75% yield). The xylene was > 99% pure by GC-MS and had a deuterium content of 97.77 atom % deuterium-d_3, 1.60 atom % deuterium-d_2, and 0.20 atom % deuterium-d_1, and 0.54% atom %

deuterium-d_0. Reactions were monitored using HPLC (Econosil C18, 5μ, 4.6 × 250 mm, 85% acetonitrile-water mixture, 1 mL/min) and standards of unlabeled compounds.

Synthesis and Characterization of m-Xylene-α-$^2H_3$

This compound was synthesized following the method described for *p*-xylene-α-$^2H_3$. The xylene was > 99% pure by GC-MS and had a deuterium content of 94.70 atom % deuterium-d_3, 4.51 atom % deuterium-d_2, 0.08 atom % deuterium-d_1, and 0.70 atom % deuterium-d_0.

Determination of Intramolecular Deuterium Isotope Effects for the Benzylic Hydroxylation of o-Xylene-α-$^2H_3$, m-Xylene-α-$^2H_3$, p-Xylene-α-$^2H_3$, 2-$^2H_3$,6-Dimethylnaphthalene, 4-2H_3,4′-Dimethylbiphenyl

Incubations contained 50 pmol CYP2E1 or CYP2A6 Supersomes in 50 mM potassium phosphate buffer (pH = 7.4). Substrate (1 mM in methanol) was added except for the biphenyl compound which was added to a final concentration of 0.5 mM. Total methanol concentration ranged from 0.8% to 1.3% (v/v). P450, buffer and substrate were pre-incubated for five minutes at 37 °C and the reaction initiated by the addition of NADPH (final concentration = 1 mM). The incubations proceeded for 30 minutes and were terminated and extracted twice with 3 mL of ice-cold pentane. The pentane layers were combined and dried with magnesium sulfate. The magnesium sulfate was removed by centrifugation and the pentane layers were evaporated to approximately 30 μL with dry N_2. Derivatization of the hydroxyl metabolites was achieved by the addition of 100 μL BSTFA/ethyl acetate (1:1) and heating at 50 °C for 30 minutes. The derivatized samples were then analyzed by GC-MS. An example of a typical chromatogram is displayed (Figure 2).

Determination of Deuterium Isotope Effects for the Benzylic Hydroxylation of p-Xylene Using a Competitive Intermolecular Design

Incubation conditions and analysis were the same as for the intramolecular experiments except that substrate consisted of a 1:1 mixture of unlabeled (d_0) and labeled (d_6; both methyl groups labeled) *p*-xylene which was added to a final total xylene concentration of 1 mM.

Quantification of Metabolic Switching for the Hydroxylation of m-Xylene-α-$^2H_3$

The products of *m*-xylene oxidation (*m*-methylbenzylalcohol and 2,4-dimethylphenol) were quantified using *p*-methylbenzylalcohol as an internal standard which was added just prior to pentane extraction. A typical standard curve for these two compounds is provided in the supplemental material. The interday coefficient of variation was < 3% for *m*-methylbenzylalcohol detection (250 pmol/mL) and < 9% for 2,4-dimethylphenol detection (50 pmol/mL).

GC-MS Analysis

Derivatized metabolites were analyzed with a Finnigan Trio 1000 mass spectrometer interfaced with a Hewlett-Packard 5890 GC equipped with a DB-5 capillary column (30 m). The column head pressure was set at 5 psi with helium used as the carrier gas. The mass spectrometer was operated in the electron impact mode (EI) at −70 eV electron energy with source and interface temperatures set at 200 °C and 250 °C, respectively. To determine the deuterium incorporation for the substrates the ionization energy was set to −12.5 eV and the GC conditions were as reported previously [18;21] except for *m*-and *p*-xylene which were injected at an oven temperature of 50 °C and held at a constant temperature for five minutes. Ions were detected in the selected ion monitoring mode (SIM). Xylene metabolites were injected on the column at an oven temperature of 40 °C, held at constant temperature for 1 minute, and eluted with a linear gradient of 3 °C/min to 180 °C. The naphthyl and biphenyl compounds were injected at an oven temperature of 130 °C, held at a constant temperature for one minute, and eluted with

a linear temperature gradient of 5 °C/min to 270 °C. Monitored ions corresponded to the $[M-15]^+$ fragments generated from the trimethylsilated hydroxyl metabolites. Confirmation of the metabolite retention times was accomplished by comparison to the retention times of synthetic or commercially available standards. Isotope effect values were calculated using the peak areas of the appropriate ions. Corrections for natural isotopic abundance and incomplete deuterium incorporation were made as previously described [18].

Results

Comparison of Intramolecular Isotope Effects for CYP2E1 and CYP2A6

The observed intramolecular isotope effects for the CYP2E1 and CYP2A6 mediated hydroxylation of a series of symmetrical, selectively deuterium-labeled substrates are presented in Table 1. The observed isotope effect is a combination of one primary isotope effect and two secondary isotope effects (PS^2). The trend in isotope effect suppression was similar for both enzymes: full k_H/k_D expression with *o*-xylene, partial suppression with *m*-xylene, *p*-xylene, and dimethylnaphthalene, and significant suppression for the biphenyl substrate. One noted difference between the isoforms was the incomplete suppression observed with oxidation of the biphenyl substrate when hydroxylated by CYP2E1 ($(k_H/k_D)_{obs} = 2.28 \pm 0.18$); the intrinsic isotope effect for this substrate was completely suppressed when submitted to CYP2A6 mediated hydroxylation ($(k_H/k_D)_{obs} = 1.07 \pm 0.07$). Interestingly, for both enzymes, the degree of suppression observed for the dimethylnaphthalene substrate was not profoundly different from the isotope effect suppression observed for *p*-xylene even though this corresponds to a rather significant difference in distance between unlabeled and labeled methyl groups.

Quantitation of Branching Observed with m-Xylene

Metabolic switching was observed for *m*-xylene hydroxylation by both isoforms. Switching (i.e., from benzylic hydroxylation to aromatic hydroxylation) was not observed for any of the other substrates. The degree of switching was quantified and is presented in Table 2. The benzylic alcohol was still the major product for both enzymes but the phenol contributed more significantly to the total product formed by CYP2A6 (16.4% total product) than by CYP2E1 (3.1%).

Intermolecular Competitive Experiment

Results for the intermolecular competitive experiment using unlabeled *p*-xylene and *p*-xylene-α, α, α, α′, α′, α′-d_6 are presented in Table 3. The strength of the intramolecular isotope effect experimental design that is used in this study relies on the assumption that the substrate is reorienting in the active site. However, theoretically, it is not necessary that a substrate reorient within the active site in order for labeled and unlabeled methyl groups to interchange. An alternative scenario is that the substrate may associate and dissociate rapidly from the enzyme [34;35]. In order to test which model is pertinent in the current system a competitive intermolecular experiment was conducted. In a competitive intermolecular experiment a 1:1 mixture of the labeled (d_6) and unlabeled (d_0) substrate is incubated with the enzyme. If substrate association and dissociation rates are rapid relative to the oxidative event then an isotope effect should be observed since the enzyme 'will choose' the substrate that is energetically more readily oxidized. However, if association/dissociation is slow relative to the oxidative event then no isotope effect should be observed ($(k_H/k_D)_{obs} = 1$). Using labeled (d_6) and unlabeled (d_0) *p*-xylene as the substrate it is apparent that the rapid interconvertible model (rapid reorientation *within* the active site) is applicable for *p*-xylene interactions with both CYP2E1 and CYP2A6 as no isotope effect was observed for this substrate mixture.

Discussion

Considering the kinetic complexities of some substrate-CYP complexes and the dynamic nature of CYPs, a combination of methods is necessary to reveal the mechanisms of substrate binding. That is, static methods, such as site-directed mutagensis and x-ray crystallography, are valuable tools in identifying residues that have a role in determining product selectivity and enzyme activity. In addition, dynamic methods are required to provide direct information about a given residue's effect on the actual motion of a substrate in the active site. Therefore, with this study we hoped to identify differences in substrate dynamics for CYP2E1 and CYP2A6; these differences could then be exploited using reciprocal mutagenesis in the future, to identify specific residues that impact not only product selectivity but also rates of substrate reorientation. Recently, a similar experimental approach was used effectively to elucidate the influence of phenylalanine 87 on substrate dynamics in $P450_{BM-3}$ [36].

Substrate dynamics were assessed by determining the observed intramolecular deuterium isotope effects associated with the benzylic hydroxylation of symmetrical, selectively deuterium labeled substrates. The extent to which the intrinsic isotope effect is expressed is dependent on the rate of reorientation of the substrates. In other words, rapid interchange between the labeled and unlabeled sites will lead to full expression of the intrinsic isotope effect. On the other hand, if the rate of reorientation is decreased (i.e., reduced rotational and/or translation motion), for example, by the residues that line the active site, then the intrinsic isotope effect will be suppressed.

It is clear from the high isotope effects observed with *o*-xylene that the interchange between labeled and unlabeled methyl groups is rapid in both CYP2E1 and CYP2A6 (Table 1). Analysis of the $(k_H/k_D)_{obs}$ suppression profiles indicate that the active sites of both enzymes are indeed rather restricted as significant suppression is observed with *m*-xylene and *p*-xylene in comparison to *o*-xylene. The metabolic switching from benzylic hydroxylation (*m*-methylbenzylalcohol formation) to aromatic hydroxylation (2, 4-dimethylphenol formation) that is observed with *m*-xylene suggests that the isotope effect values observed for this substrate, especially for CYP2A6, might be elevated to some degree since oxidation at an alternate site can unmask the intrinsic isotope effect [19;37]. The suppression observed with the *m*- and *p*-xylene substrates indicates that reorientation is partially hindered for these substrates in both CYP2E1 and CYP2A6. Therefore, the spatial limits to unhindered substrate reorientation can be estimated; this assumes that only one xylene molecule is bound to the enzyme. Based on the distances between methyl groups, which were determined using molecular modeling, the spatial limits to unhindered substrate reorientation are in the range of 7 $Å^2$ to 27 $Å^2$ and 14 $Å^3$ to 103 $Å^3$ for two-dimensional and three-dimensional motion, respectively.

Overall, only minor differences were observed in the suppression profiles for CYP2E1 and CYP2A6 especially compared to the differences observed in previous comparative studies that utilized the same technique [21;36]. For two enzymes with a broad overlap in substrate selectivity it is not especially surprising that they would display similar isotope effect suppression profiles and that the observed differences in product selectivity in certain cases could be due to subtle differences in the respective active sites.

Interestingly, for two enzymes that selectively oxidize 'smaller' substrates, the isotope effect suppression for the naphthyl compound, although statistically significant, was not profoundly different from the $(k_H/k_D)_{obs}$ for *p*-xylene (6.04 ± 0.26 versus 5.50 ± 0.47 for CYP2E1 and 5.53 ± 0.19 versus 4.96 ± 0.22 for CYP2A6; $p < 0.01$ and $p < 0.0004$ for CYP2E1 and CYP2A6, respectively). Since the observed isotope effect is dependent on the rate of interchange of protio and deutero sites these minor differences in $(k_H/k_D)_{obs}$ suggest that the interchange rates for

these two substrates are similar even though these compounds span a notable difference in area (27 $Å^2$ to 51 $Å^2$) and volume (103 $Å^3$ to 271 $Å^3$). Since the intrinsic isotope effects for both substrates (and isoforms) are only partially suppressed, both substrates rotate rapidly in the enzyme active sites relative to the rate of substrate oxidation, since the labeled and unlabeled sites must interchange rapidly in order for an isotope effect to be observed. In the case of *p*-xylene this interchange must be occurring within the active since no isotope effect was observed when the intermolecular competitive isotope effect experiment was conducted using a 1:1 mixture of unlabeled (d_0) and labeled (d_6) *p*-xylene. This would mean that *p*-xylene and dimethylnaphthalene reorient at approximately the same rate even though dimethylnaphthalene is much larger than *p*-xylene and should take up more of the active site volume. That is, theoretically, the enzyme active site structure should hinder dimethylnaphthalene dynamics to a greater extent in comparison to *p*-xylene.

One explanation for only minor differences in isotope effect suppression in the face of a large increase in spatial requirement is that CYP2A6 and CYP2E1 have some flexibility and may undergo conformational changes to accommodate the larger naphthyl substrate. These conformational changes would provide, on average, a 'roomier' active site that allows the protio/deutero interchange rate to be maintained in going from *p*-xylene to dimethylnaphthalene. This is consistent with other studies where it has been shown that CYP2E1 flexibility can be modulated by different substrates [8]. In the case of CYP2A6, the x-ray crystal structure indicates that it has a restricted active site (260 $Å^3$) that requires a conformational change to allow the coumarin substrate to enter the active site [38]. The observation that the intrinsic isotope effect is not completely suppressed for the CYP2E1 mediated hydroxylation of dimethylbiphenyl ($k_H/k_D = 2.28$) also provides some support for the conformational change explanation. That is, CYP2E1 must be accommodating enough to allow at least some reorientation of this relatively large substrate, albeit at a significantly reduced rate; whether this reorientation occurs within the active site (a non-dissociative mechanism) or through a dissociative mechanism is not clear without further experimentation. Alternatively, uncoupling may produce an increased observed isotope effect which, in the absence of this branching process, might be completely suppressed [19;39]

There is another explanation for the minor differences in isotope effect suppression observed for *p*-xylene compared to dimethylnaphthalene. Hypothetically, the $(k_H/k_D)_{obs}$ values observed for the xylene substrates could be generated by the presence of two substrates bound simultaneously to the CYP instead of a single xylene molecule. That is, k_H/k_D suppression (i.e., decreased substrate reorientation rates) with some of the xylene isomers could be caused by substrate-substrate interactions in addition to interactions with the enzyme active site structure. Considering the relatively high substrate concentrations used for the experiments (1 mM) this latter scenario seems plausible.

In summary, it is evident that substrate binding for P450 enzymes involves varying degrees of protein dynamics [5;6;7;8;38]. This flexibility to accommodate various substrates appears to be an effective and economical characteristic considering the myriad of exogenous compounds that an organism must oxidize and clear from the system. The strength of intramolecular isotope effect experiments is that they can provide information regarding the dynamics of *substrates* in the active site. Assuming a single substrate is interacting with each enzyme, the data presented here for *p*-xylene and dimethylnaphthalene could be interpreted to indicate enzyme structural dynamics based on the similar orientation rates for these two substrates that differ significantly in size. On the other hand, in some cases it is possible that $(k_H/k_D)_{obs}$ is the result of multiple substrates (e.g., two *p*-xylene molecules) bound to the enzyme simultaneously. If this latter case is applicable in some instances, then intramolecular isotope effect experiments should be especially valuable in the mechanistic investigation of P450 cooperativity, which

was recently proposed [20]. Experiments that address this hypothesis will be addressed elsewhere.

On a final note, CYP2E1 and CYP2A6 displayed different degrees of product selectivity for d_3-*m*-xylene oxidation (Table 2). Therefore d_3-*m*-xylene may represent a new probe substrate for additional comparative structural studies between CYP2E1 and CYP2A6.

Supplementary Material

Refer to Web version on PubMed Central for supplementary material.

References

1. Vaz AD, Pernecky SJ, Raner GM, Coon MJ. Peroxo-iron and oxenoid-iron species as alternative oxygenating agents in cytochrome P450-catalyzed reactions: switching by threonine-302 to alanine mutagenesis of cytochrome P450 2B4. Proc Natl Acad Sci U S A 1996;93:4644–8. [PubMed: 8643457]
2. Spatzenegger M, Liu H, Wang Q, Debarber A, Koop DR, Halpert JR. Analysis of differential substrate selectivities of CYP2B6 and CYP2E1 by site-directed mutagenesis and molecular modeling. J Pharmacol Exp Ther 2003;304:477–87. [PubMed: 12490624]
3. Khan KK, He YQ, Domanski TL, Halpert JR. Midazolam oxidation by cytochrome P450 3A4 and active-site mutants: an evaluation of multiple binding sites and of the metabolic pathway that leads to enzyme inactivation. Mol Pharmacol 2002;61:495–506. [PubMed: 11854429]
4. Domanski TL, He YA, Harlow GR, Halpert JR. Dual role of human cytochrome P450 3A4 residue Phe-304 in substrate specificity and cooperativity. J Pharmacol Exp Ther 2000;293:585–91. [PubMed: 10773032]
5. Williams PA, Cosme J, Ward A, Angove HC, Matak Vinkovic D, Jhoti H. Crystal structure of human cytochrome P450 2C9 with bound warfarin. Nature 2003;424:464–8. [PubMed: 12861225]
6. Scott EE, He YA, Wester MR, White MA, Chin CC, Halpert JR, Johnson EF, Stout CD. An open conformation of mammalian cytochrome P450 2B4 at 1.6-A resolution. Proc Natl Acad Sci U S A 2003;100:13196–201. [PubMed: 14563924]
7. Scott EE, White MA, He YA, Johnson EF, Stout CD, Halpert JR. Structure of mammalian cytochrome P450 2B4 complexed with 4-(4-chlorophenyl)imidazole at 1.9-A resolution: insight into the range of P450 conformations and the coordination of redox partner binding. J Biol Chem 2004;279:27294–301. [PubMed: 15100217]
8. Smith SV, Koley AP, Dai R, Robinson RC, Leong H, Markowitz A, Friedman FK. Conformational modulation of human cytochrome P450 2E1 by ethanol and other substrates: a CO flash photolysis study. Biochemistry 2000;39:5731–7. [PubMed: 10801323]
9. Prasad S, Mazumdar S, Mitra S. Binding of camphor to Pseudomonas putida cytochrome p450(cam): steady-state and picosecond time-resolved fluorescence studies. FEBS Lett 2000;477:157–60. [PubMed: 10908713]
10. Prasad S, Mitra S. Role of protein and substrate dynamics in catalysis by Pseudomonas putida cytochrome P450cam. Biochemistry 2002;41:14499–508. [PubMed: 12463748]
11. Davydov DR, Botchkareva AE, Kumar S, He YQ, Halpert JR. An electrostatically driven conformational transition is involved in the mechanisms of substrate binding and cooperativity in cytochrome P450eryF. Biochemistry 2004;43:6475–85. [PubMed: 15157081]
12. Jovanovic T, McDermott AE. Observation of ligand binding to cytochrome P450 BM-3 by means of solid-state NMR spectroscopy. J Am Chem Soc 2005;127:13816–21. [PubMed: 16201802]
13. Lee H, Ortiz de Montellano PR, McDermott AE. Deuterium magic angle spinning studies of substrates bound to cytochrome P450. Biochemistry 1999;38:10808–13. [PubMed: 10451377]
14. Foster AB, Jarman M, Stevens JD, Thomas P, Westwood JH. Isotope effects in O- and N-demethylations mediated by rat liver microsomes: an application of direct insertion electron impact mass spectrometry. Chem Biol Interact 1974;9:327–40. [PubMed: 4434564]
15. Hamberg M, Bjorkhem I. -Oxidation of fatty acids. I. Mechanism of microsomal 1- and 2-hydroxylation. J Biol Chem 1971;246:7411–6. [PubMed: 5135309]

16. Hjelmeland LM, Aronow L, Trudell JR. Intramolecular determination of substituent effects in hydroxylations catalyzed by cytochrome P-450. Mol Pharmacol 1977;13:634–9. [PubMed: 887073]
17. Nelson SD, Trager WF. The use of deuterium isotope effects to probe the active site properties, mechanism of cytochrome P450-catalyzed reactions, and mechanisms of metabolically dependent toxicity. Drug Metab Dispos 2003;31:1481–98. [PubMed: 14625345]
18. Iyer KR, Jones JP, Darbyshire JF, Trager WF. Intramolecular isotope effects for benzylic hydroxylation of isomeric xylenes and 4,4′-dimethylbiphenyl by cytochrome P450: relationship between distance of methyl groups and masking of the intrinsic isotope effect. Biochemistry 1997;36:7136–43. [PubMed: 9188713]
19. Korzekwa KR, Trager WF, Gillette JR. Theory for the observed isotope effects from enzymatic systems that form multiple products via branched reaction pathways: cytochrome P-450. Biochemistry 1989;28:9012–8. [PubMed: 2605238]
20. Atkins WM. Non-Michaelis-Menten kinetics in cytochrome P450-catalyzed reactions. Annu Rev Pharmacol Toxicol 2005;45:291–310. [PubMed: 15832445]
21. Henne KR, Fisher MB, Iyer KR, Lang DH, Trager WF, Rettie AE. Active site characteristics of CYP4B1 probed with aromatic ligands. Biochemistry 2001;40:8597–605. [PubMed: 11456500]
22. Chang TK, Gonzalez FJ, Waxman DJ. Evaluation of triacetyloleandomycin, alpha-naphthoflavone and diethyldithiocarbamate as selective chemical probes for inhibition of human cytochromes P450. Arch Biochem Biophys 1994;311:437–42. [PubMed: 8203907]
23. Draper AJ, Madan A, Parkinson A. Inhibition of coumarin 7-hydroxylase activity in human liver microsomes. Arch Biochem Biophys 1997;341:47–61. [PubMed: 9143352]
24. Pelkonen O, Rautio A, Raunio H, Pasanen M. CYP2A6: a human coumarin 7-hydroxylase. Toxicology 2000;144:139–47. [PubMed: 10781881]
25. Patten CJ, Ishizaki H, Aoyama T, Lee M, Ning SM, Huang W, Gonzalez FJ, Yang CS. Catalytic properties of the human cytochrome P450 2E1 produced by cDNA expression in mammalian cells. Arch Biochem Biophys 1992;299:163–71. [PubMed: 1444447]
26. Shimada T, Tsumura F, Yamazaki H. Prediction of human liver microsomal oxidations of 7-ethoxycoumarin and chlorzoxazone with kinetic parameters of recombinant cytochrome P-450 enzymes. Drug Metab Dispos 1999;27:1274–80. [PubMed: 10534312]
27. Spracklin DK, Hankins DC, Fisher JM, Thummel KE, Kharasch ED. Cytochrome P450 2E1 is the principal catalyst of human oxidative halothane metabolism in vitro. J Pharmacol Exp Ther 1997;281:400–11. [PubMed: 9103523]
28. Spracklin DK, Kharasch ED. Human halothane reduction in vitro by cytochrome P450 2A6 and 3A4: identification of low and high KM isoforms. Drug Metab Dispos 1998;26:605–7. [PubMed: 9616199]
29. Yoo JS, Ishizaki H, Yang CS. Roles of cytochrome P450IIE1 in the dealkylation and denitrosation of N-nitrosodimethylamine and N-nitrosodiethylamine in rat liver microsomes. Carcinogenesis 1990;11:2239–43. [PubMed: 2265475]
30. Le Gal A, Dreano Y, Lucas D, Berthou F. Diversity of selective environmental substrates for human cytochrome P450 2A6: alkoxyethers, nicotine, coumarin, N-nitrosodiethylamine, and N-nitrosobenzylmethylamine. Toxicol Lett 2003;144:77–91. [PubMed: 12919726]
31. Feierman DE, Cederbaum AI. Inhibition of microsomal oxidation of ethanol by pyrazole and 4-methylpyrazole in vitro. Increased effectiveness after induction by pyrazole and 4-methylpyrazole. Biochem J 1986;239:671–7. [PubMed: 3827819]
32. Guengerich FP, Kim DH, Iwasaki M. Role of human cytochrome P-450 IIE1 in the oxidation of many low molecular weight cancer suspects. Chem Res Toxicol 1991;4:168–79. [PubMed: 1664256]
33. Chen W, Koenigs LL, Thompson SJ, Peter RM, Rettie AE, Trager WF, Nelson SD. Oxidation of acetaminophen to its toxic quinone imine and nontoxic catechol metabolites by baculovirus-expressed and purified human cytochromes P450 2E1 and 2A6. Chem Res Toxicol 1998;11:295–301. [PubMed: 9548799]
34. Gillette JR, Darbyshire JF, Sugiyama K. Theory for the observed isotope effects on the formation of multiple products by different kinetic mechanisms of cytochrome P450 enzymes. Biochemistry 1994;33:2927–37. [PubMed: 8130206]

35. Darbyshire JF, Gillette JR, Nagata K, Sugiyama K. Deuterium isotope effects on Aring and D-ring metabolism of testosterone by CYP2C11: evidence for dissociation of activated enzyme-substrate complexes. Biochemistry 1994;33:2938–44. [PubMed: 8130207]

36. Rock DA, Boitano AE, Wahlstrom JL, Rock DA, Jones JP. Use of kinetic isotope effects to delineate the role of phenylalanine 87 in P450(BM-3). Bioorg Chem 2002;30:107–18. [PubMed: 12020135]

37. Jones JP, Korzekwa KR, Rettie AE, Trager WF. Isotopically Sensitive Branching and Its Effect on the Observed Intramolecular Isotope Effects in Cytochrome P-450 Catalyzed Reactions: A New Method for the Estimation of Intrinsic Isotope Effects. J Am Chem Soc 1986;108:7074–7078.

38. Yano JK, Hsu MH, Griffin KJ, Stout CD, Johnson EF. Structures of human microsomal cytochrome P450 2A6 complexed with coumarin and methoxsalen. Nat Struct Mol Biol 2005;12:822–3. [PubMed: 16086027]

39. Atkins WM, Sligar SG. Metabolic Switching in Cytochrome P-450Cam: Deuterium Isotope Effects on Regiospecificity and the Monooxygenase/Oxidase Ratio. J Am Chem Soc 1987;109:3754–3760.

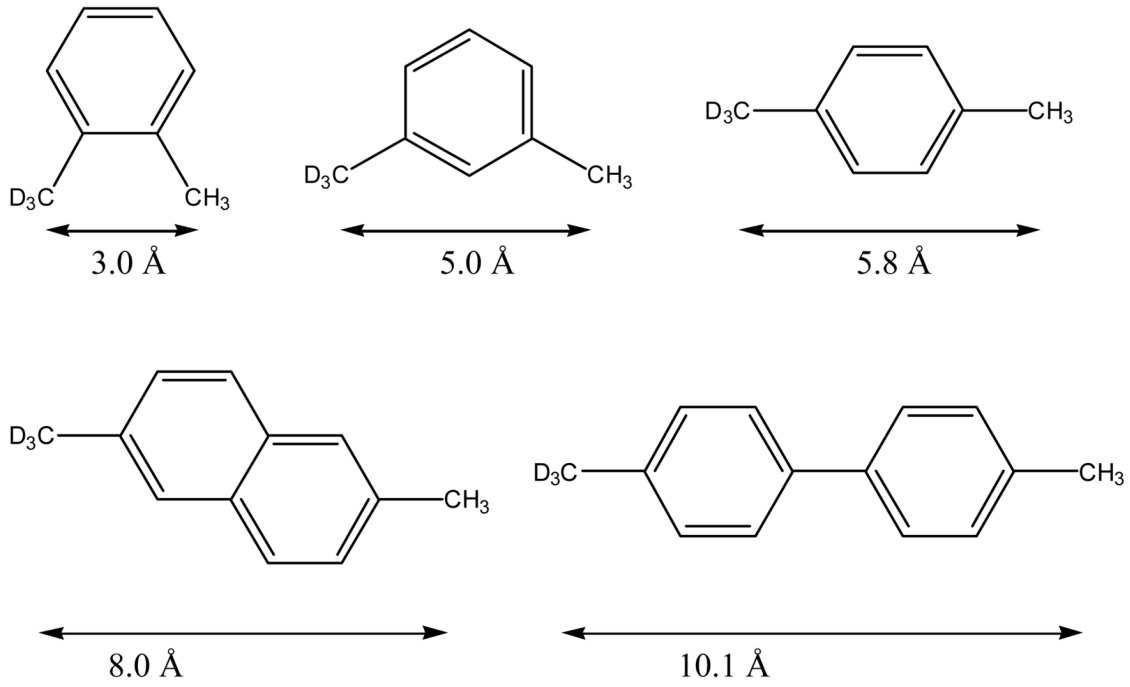

Figure 1.

Distances between methyl carbons in selectively deuterium labeled substrates used to assess substrate dynamics and active site space. The corresponding areas and volumes referenced in the text were determined by assuming a radius equal to one-half the given distances. Measurements are theoretical distances determined using Spartan Wavefunction software.

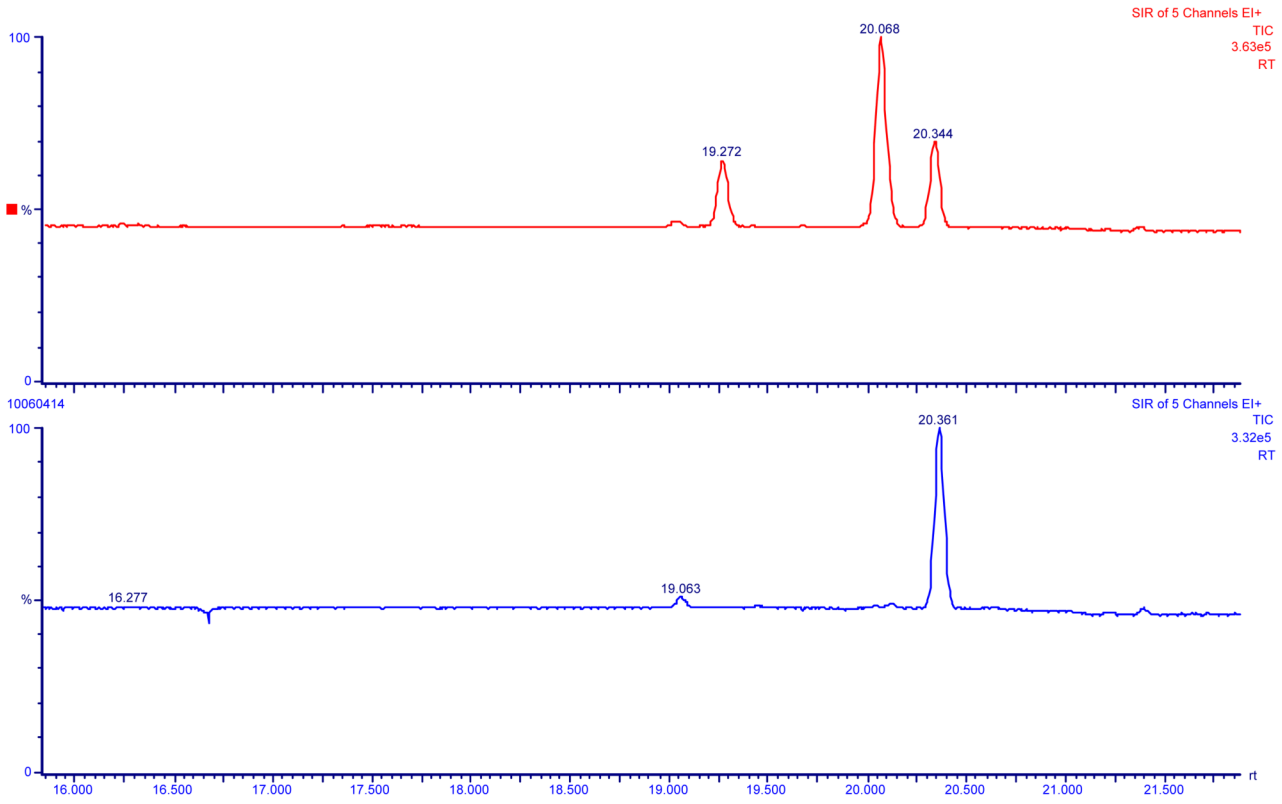

Figure 2.

Typical chromatogram for the CYP2A6-catalyzed oxidation of *m*-xylene-α -$^{2}H_{3}$ (top panel: incubation with CYP2A6; bottom panel: control with no enzyme). Retention times: 2,4-dimethylphenol (19.272 min.); *m*-methylbenzylalcohol (20.068 min).

Table 1

The observed intramolecular isotope effects for the CYP2E1 and CYP2A6 catalyzed benzylic oxidation of symmetrical deuterium-labeled substrates and the associated spatial values for two-dimensional and three-dimensional substrate motion. Numbers in parentheses indicate the number of determinations.

	(k_H/k_D)obs		Corresponding Space	
Substrate	**CYP2E1**	**CYP2A6**	**Area ($Å^2$)**	**Volume ($Å^3$)**
o-xylene-α -$^2H_3$	9.03 ± 0.42 (3)	11.46 ± 0.28 (3)	7	14
m-xylene-α -$^2H_3$	6.65 ± 0.29 (11)	7.21 ± 0.43 (8)	20	67
p-xylene-α -$^2H_3$	6.04 ± 0.26 (9)	5.53 ± 0.19 (7)	27	103
2-$^2H_3$, 6-Dimethyl- naphthalene[a]	5.50 ± 0.47 (9)	4.96 ± 0.22 (6)	51	271
4-$^2H_3$, 4′-dimethyl- biphenyl	2.28 ± 0.18 (3)	1.07 ± 0.07 (3)	81	545

[a] $p < 0.01$ and $p < 0.0004$ compared to *p*-xylene values for CYP2E1 and CYP2A6, respectively

Table 2

Quantitation of metabolic switching (benzylic versus aromatic oxidation) observed for CYP2E1 and CYP2A6 mediated hydroxylation of d_3-*m*-xylene.

	% Products		Ratio
Enzyme	**MBA**[a]	**DMP**[b]	**(MBA/DMP)**
CYP2E1	96.9 ± 0.3 (6)	3.1 ± 0.3	31.5
CYP2A6	83.6 ± 0.7 (3)	16.4 ± 0.7	5.1

[a] *m*-methylbenzylalcohol.

[b] 2,4-dimethylphenol. Number in parenthesis indicates the number of determinations

Table 3

Observed k_H/k_D for CYP2E1 and CYP2A6 mediated benzylic hydroxylation of *p*-xylene using a competitive intermolecular experimental design. Number in parenthesis indicates the number of determinations.

Enzyme	$(k_H/k_D)_{obs}$
CYP2E1	1.07 ± 0.06 (3)
CYP2A6	1.21 ± 0.03 (3)